Front. Optoelectron.
https://doi.org/10.1007/s12200-017-0764-y

REVIEW ARTICLE

Development of Bi/Er co-doped optical fibers for ultra-broadband photonic applications

Yanhua LUO (✉)[1,2], Binbin YAN[3], Jianzhong ZHANG[4], Jianxiang WEN[2], Jun HE[5], Gang-Ding PENG (✉)[1]

1 Photonics & Optical Communications, School of Electrical Engineering, University of New South Wales, Sydney 2052, NSW, Australia
2 Key Laboratory of Specialty Fiber Optics and Optical Access Networks, Shanghai University, Shanghai 200072, China
3 State Key Laboratory of Information Photonics and Optical Communications, Beijing University of Posts and Telecommunications, Beijing 100876, China
4 Key Lab of In-fiber Integrated Optics, Ministry of Education, Harbin Engineering University, Harbin 150001, China
5 Key Laboratory of Optoelectronic Devices and Systems of Ministry of Education and Guangdong Province, College of Optoelectronic Engineering, Shenzhen University, Shenzhen 518060, China

Abstract Targeting the huge unused bandwidth (BW) of modern telecommunication networks, Bi/Er co-doped silica optical fibers (BEDFs) have been proposed and developed for ultra-broadband, high-gain optical amplifiers covering the 1150–1700 nm wavelength range. Ultra-broadband luminescence has been demonstrated in both BEDFs and bismuth/erbium/ytterbium co-doped optical fibers (BEYDFs) fabricated with the modified chemical vapor deposition (MCVD) and *in situ* doping techniques. Several novel and sophisticated techniques have been developed for the fabrication and characterization of the new active fibers. For controlling the performance of the active fibers, post-treatment processes using high temperature, γ-radiation, and laser light have been introduced. Although many fundamental scientific and technological issues and challenges still remain, several photonic applications, such as fiber sensing, fiber gratings, fiber amplification, fiber lasers, etc., have already been demonstrated.

Keywords Bi/Er co-doped optical fiber (BEDF), broadband emission, bismuth-related active center (BAC), modified chemical vapor deposition (MCVD), fiber amplifier, fiber sensing

1 Introduction

With the development of the Internet, optical communication technology has been advancing rapidly, supporting our increasingly information-driven society and economy. Over the past 40 years, a series of technological breakthroughs have allowed the transmission capacity of fibers to increase ~10-fold every four years. Transmission technology has thus far been able to keep up with the steady exponential growth in the Internet protocol traffic [1]. However, the demand for higher transmission capacity will further increase, with the growth of the information demand at 30%–40% per year [2]. When the capacity of optical fibers approaches its limit, without any further innovation, increasing the total transmission capacity of a system will be possible only by using parallel fibers, which will lead to linear scaling of the associated costs and power consumption with capacity and constrain its growth. Therefore, the telecommunication research community has already started to explore the technology-driven solutions in response to the forecasted upcoming "capacity crunch" [3]. Different technologies have been exploited to increase the transmission capacity, based on different configurations and types of optical fibers, such as a parallel single-mode fiber (SMF) system sharing common amplifiers to simultaneously amplify multiple fibers within a bundle, spatial division multiplexing based on multicore or/and multimode fibers, and hollow-core fibers with ultra-low loss at ~2 μm based on thulium- and holmium-doped fiber amplifiers [3].

Apart from the technologies mentioned above, are there any other ways to deal with the forecasted upcoming "capacity crunch"? The answer is yes. With the development of water-free fiber technology, all wave silica fibers have been developed with high transmission from 1150 to 1700 nm. Wideband and flat-gain amplifiers are still necessary for wavelength division multiplexing (WDM) and dense wavelength division multiplexing (DWDM) transmission systems. However, to date, only a small

Received October 11, 2017; accepted November 3, 2017

E-mails: yanhua.luo1@unsw.edu.au, g.peng@unsw.edu.au

portion of the available spectrum has been commercially exploited for photonic networks because of the limited spectral range of the erbium-doped fiber amplifier (EDFA) operation of only 1530–1610 nm (C- and L-bands). The O- (1260–1360 nm), E- (1360–1440 nm), S^+- (1440–1460 nm), and S- (1460–1530 nm) bands are not yet fully utilized [2]. If a single amplifier could cover the entire range of available bandwidths (BWs), then the associated accessories and cost will be greatly reduced. Hence, the unavailability of suitable fiber lasers and amplifiers in the desirable bands has become the main obstacle. Although some amplifiers have been reported to operate in these bands, for example, Raman amplifiers and semiconductor optical amplifiers (SOAs), they all have limitations. For Raman amplifiers, high pump powers (1 W) are often required to achieve a gain of 20–30 dB, and several pump sources are needed for large BW. SOAs often run with low powers and have high noise, low gain, and much higher nonlinear distortion [4]. Therefore, developing suitable active fibers with ultra-broadband, high-gain amplification in the O-, E-, S-, C-, L-, and U-bands between 1150 and 1700 nm can create new applications and opportunities. It is important not only for WDM-based fiber communication but also for fiber sensing.

In this paper, we give an overview of the development of active fibers with ultra-broadband emission in the O-, E-, S-, C-, L-, and U-bands based on the bismuth/erbium co-doped optical fiber (BEDF). The technology roadmap of the BEDF development is shown in Fig. 1. According to the roadmap in Fig. 1, this paper focuses on six areas to describe the research and development of BEDFs. In Section 2.1, the material design and structure modeling of active fibers is presented. In Section 2.2, we describe fabrication of BEDFs and BEYDFs based on combined techniques of MCVD and *in situ* doping, as well as bismuth-doped optical fibers (BDFs) based on the MCVD and atomic layer deposition (ALD) techniques. In Section 2.3, several new techniques are introduced for characterization of the active fibers, especially focusing on the characterization of the ultra-broadband properties of BEDFs. In Section 2.4, the developed active fibers are assessed based on the results obtained. In Section 2.5, with the aim to improve the properties, BEDFs are treated with high temperature, gamma radiation, and laser exposure. Finally, some photonic applications of BEDFs are demonstrated, and the results are evaluated in Section 2.6.

2 BEDF development

2.1 Material design and considerations

2.1.1 Ultra-broadband spectrum by Bi/Er and Bi/Er/Yb co-doping

Water-free fiber technology has enabled silica fibers to achieve ultra-broadband low-loss transmission in the wavelength range of 1000–1750 nm (1200–1700 nm), where the optical losses of the transmission fibers are less than 1 dB/km (0.5 dB/km) (Fig. 2) [2]. The spectral ranges of the most efficient active media based on rare-earth-doped fibers are demonstrated in Fig. 2 for the near infrared (NIR) region [2]. Figure 2 clearly indicates that it is impossible to construct efficient optical amplifiers based on rare-earth-doped optical fibers for the extended bands. Although considerable interest has previously been attracted to fiber amplifiers and fiber lasers based on fibers doped with rare-earth ions, e.g., Yb^{3+}, Nd^{3+}, Er^{3+}, Tm^{3+}, Ho^{3+}, and Pr^{3+}, for the extended bands, none of them demonstrated sufficient optical gain and BW for practical applications in fiber telecommunication networks.

In recent years, significant research efforts have been

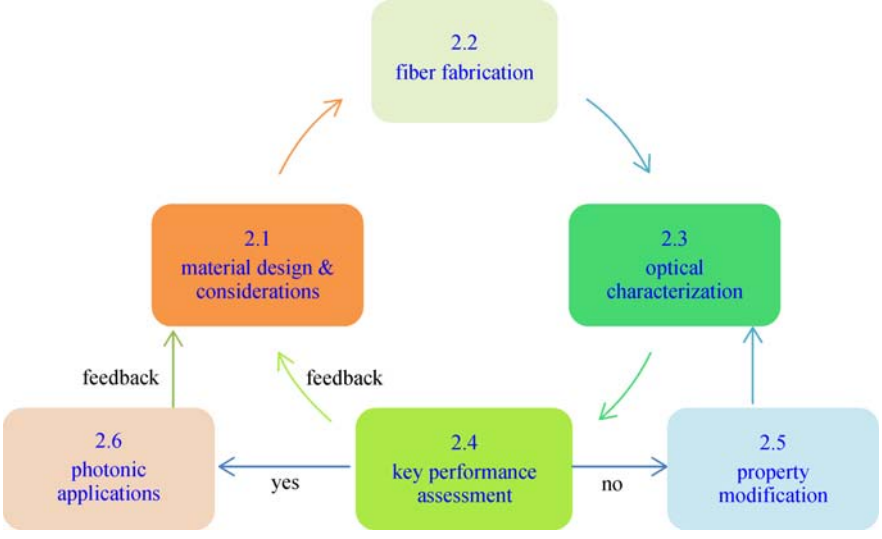

Fig. 1 Technology roadmap of BEDF development

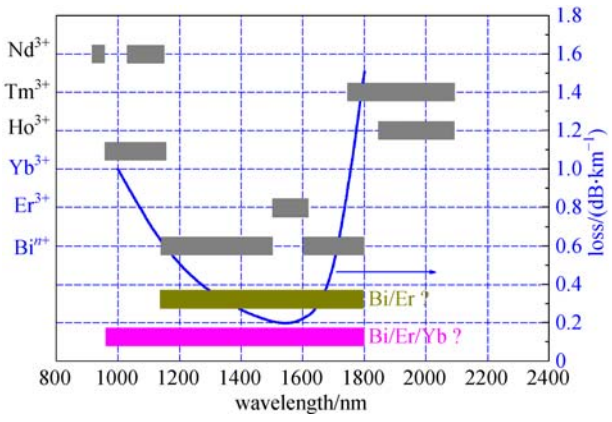

Fig. 2 Spectral ranges of various doping elements as well as the low-loss spectrum of silica-based optical fibers

devoted to optical glasses or materials with Bi-doping for the extended band [5–10], since the first demonstration of broadband NIR luminescence in Bi-doped silica glass in 1999 [11]. The development of these materials has spurred a significant amount of works on the associated optical fibers [2,12,13] since the first fabrication of BDFs in 2005 [14]. In the past decade, studies have demonstrated that BDFs are promising active media for the NIR spectral region from 1150 to 1800 nm, including the regions from 1250 to 1500 nm and 1600 to 1800 nm (Fig. 2), where efficient rare-earth-doped fiber lasers are absent [15,16].

Therefore, Bi/Er [17–20] and Bi/Er/Yb co-doped glasses have been proposed to cover the O-, E-, S-, C- and L-bands, as shown in Fig. 2, in order to fully utilize the telecommunications transmission window in the range of 1000–1700 nm. Kuwada et al. [17] reported ultra-broadband fluorescence between 1160 and 1570 nm from a Bi/Er co-doped bulk silica glass prepared by melt mixing in a crucible. Peng et al. [18] reported ultra-broadband fluorescence between 1160 and 1580 nm from Bi/Er co-doped germinate glasses. Furthermore, Minh Hau et al. [19] reported ultra-broadband fluorescence between 1130 and 1580 nm from Bi/Er co-doped lanthanum aluminosilicate glasses. An extremely broadband emission between 1190 and 1920 nm has also been observed in Bi/Er/Tm co-doped lanthanum aluminosilicate glasses [20]. Extending that idea, we succeeded to develop the first Bi/Er co-doped fibers (BEDFs) with broad emission between 1100 and 1570 nm in 2012 [21] and the first Bi/Er/Yb co-doped fibers with even broader emission between 1000 and 1590 nm in 2015 [22].

2.1.2 Nature and structure of bismuth-related active centers (BACs)

Despite the great success in the development of BEDFs with ultra-broadband emission in the second and third telecommunication windows, many fundamental scientific and technological issues and challenges remain before BEDFs can be practically and commercially used in fiber lasers and amplifiers. One key challenge is that the nature of BACs is not clear [15]. Therefore, one task in the development of BEDFs is to explore the structure of BACs, so that we can easily optimize the ultra-broadband emission and its efficiency through controlling the material composition and fabrication conditions. In our previous work, using the density functional theory in quantum-chemical calculations, energy levels associated with structural models of different valence states of Bi ions have been investigated in Bi-doped silica fibers [23]. In particular, the local structure models (e.g., in Fig. 3) of Bi^{5+}, Bi^{3+}, and Bi^{+} with and without Al ions have been analyzed and compared with respect to their fluorescence characteristics. The results reveal that the NIR emission possibly comes from Bi^{5+} and/or Bi^{3+}. In particular, Bi^{5+} may combine with Al ions that activate the luminescence center of Bi^{5+}, resulting in the distinctive fluorescence related to coupling between Bi^{5+} and Al^{3+}. In addition, the NIR fluorescence may come from the Al-free Bi^{3+} ions.

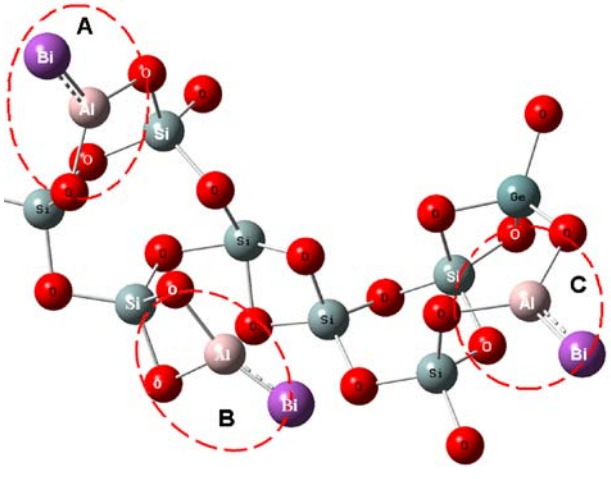

Fig. 3 Local structure model of Bi-doping into the distinct sites among the silica-based network microstructure (A, B, C)

Fluorescence from Bi^{+} may exist, but its contribution to the total fluorescence signal is nominal. These preliminary theoretical results indicate that the properties of the NIR emission are related to the complexity of BACs.

In fact, difficulties arise from the fact that Bi is a transition metal with *d* orbitals that are easily coupled to the surrounding environment, unlike the rare-earth elements that have well-isolated *f*–*f* transitions. On the other hand, it is this coupling to the external environment that allows tailoring the formation of broadband emission defect sites using additional dopants such as aluminum, germanium, phosphorous, etc. As "the wonder metal," bismuth can participate in numerous reduction reactions without other elements, producing a variety of products [24]. With the increasing melting temperature of Bi-doped glasses, the following change in the valence state of bismuth takes place [25]: $Bi^{3+} \rightarrow Bi^{2+} \rightarrow Bi^{+} \rightarrow Bi/Bi_2$, Bi_2^{-}, Bi_3, etc., $\rightarrow (Bi)_n$, where Bi_2, Bi_2^{-}, Bi_3, etc. are Bi clusters, and $(Bi)_n$ is a metallic colloid. So far, a number of hypotheses have been suggested for the origin of the NIR emission from Bi-doped glasses [10] like Bi^{+}, Bi^{5+}, Bi-clusters, BiO, Bi^{2-}, Bi_2^{2-} point defects, etc., but none of them have been experimentally confirmed. Sun et al. revealed that Bi_5^{3+} [26], Bi_8^{2+} [27], and Bi_2^{2-} [28] in molecular crystals and Bi^{+} in zeolites [29] are NIR emitters, but whether these emitters exist in glassy systems such as bulk glasses or fibers remains an open question for further investigation. Even the latest experimental data obtained from Bi-doped germanosilicate fibers with a small concentration of Bi ($\leqslant$0.1 at.%) can only confirm that BACs are clusters consisting of Bi ions and oxygen deficiency centers but not Bi ions themselves [15]. However, the structural configurations and the type of Bi ions forming BACs are still unclear.

It is known that fiber preform fabrication involves ultra-high temperatures, while fiber drawing involves ultra-high temperatures and fast annealing. These processes give the possibility of the formation of multiple valence states of bismuth, as well as defects. These processes also hint that BACs should be related mainly to lower-valent bismuth, such as Bi^{0} or Bi^{+} [30] instead of higher-valent bismuth (Bi^{3+} and Bi^{5+}). In addition, the existence of NIR luminescence from Bi that was doped in $AlCl_3$–NaCl eutectic liquid, fluoride glass, chloride glass, and chalcogenide also indicates that the presence of oxygen is not prerequisite [10]. Therefore, it is believed that BACs that cause NIR luminescence are formed mostly from the lower-valent bismuth, as well as some type of defects.

2.1.3 Material composition and spectral considerations

The coupling of bismuth to its external environment results in strong influence of local environment on the properties of BACs. According to the types of local environment, there are four types of BACs: BAC-Si, BAC-Ge, BAC-Al, and BAC-P, which are closely linked to their specific sites: SiO_2, GeO_2, P_2O_5:SiO_2, and Al_2O_3:SiO_2, respectively [31,32]. The normalized luminescence spectra of fibers associated with these BACs are displayed in Fig. 4, together with those of Er^{3+}- and Yb^{3+}-doped optical fibers [31–34]. As seen from Fig. 4, these active centers cover different bands from 900 to 1850 nm and have different spectral profiles. One can, therefore, achieve ultra-broadband emission from 1000 to 1800 nm by corresponding co-doping.

It is interesting to note that efficient gains and lasing in BDFs were only observed in optical fibers with a low concentration of bismuth. The concentration of BACs initially grows with the increasing bismuth concentration; however, with further increase of the bismuth concentration, the growth of the BAC concentration is slower than the growth of the optical background losses in BDFs [35]. Therefore, to produce the desirable broadband emission, the Bi concentrations of both BDFs and BEDFs should be low ($<$0.1 mol%) [2,15,21,36,37]. In addition, an ultra-high concentration of bismuth will transform BEDFs into Bi-glass-based Er-doped fibers (usually referred to as Bi-EDFs or B-EDFs) [38]. These Bi-EDFs have very high Bi concentrations ($>$50 mol%), totally different from the targeted BEDFs. In these Bi-EDFs, Bi glasses are often used as host materials only for improving the Er emission in C- and L-bands, and their emission characteristics are totally different from BEDFs for broadband emission covering all (O-, E-, S-, C-, and L-) bands. Therefore, although the emission of BEDFs can easily cover the combined extended bands from 1000 to 1700 nm, due to the differences in emission efficiency and spectral profiles (Fig. 4), as well as possible energy transfer between them, the optimization of the material composition and fabrication techniques to achieve broad, high, and flat luminescence and gain is a big challenge.

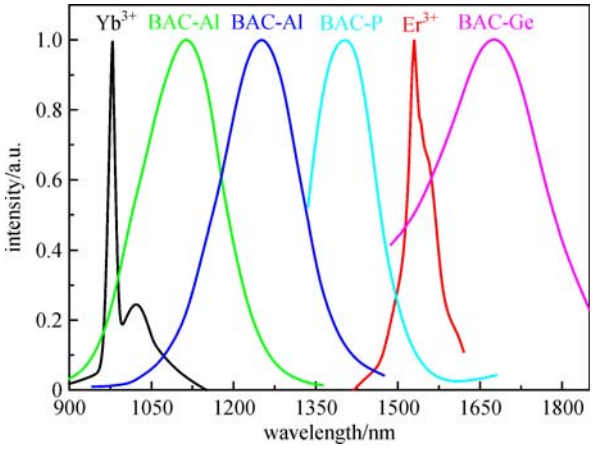

Fig. 4 Normalized luminescence spectra of erbium-doped optical fiber (EDF), ytterbium-doped optical fiber (YDF), and various BDFs [31–34]

2.2 Fiber fabrication

2.2.1 BEDF fabrication by MCVD and the *in situ* doping technique

Following the proposed idea, the first BEDF was fabricated using MCVD combined with the in situ doping technique at the Joint National Fiber Facility at The University of New South Wales (Fig. 5(a)) [39]. First, the inner layer is etched with SF_6, and then undoped silica cladding layers (P, F or Ge, Si) are deposited at 1800°C in the standard manner. For the core layer, an undoped soot layer (P, Ge, Si) is deposited at 1600°C. The soot is then presintered at ~1200°C to ensure good strength. Instead of removing the substrate tube from the lathe, dopants are introduced into the porous soot with the in situ doping technique, which can reduce the processing time and increase the dopant concentration as compared to the conventional solution doping [40]. After the drying process, the doped soot layer is consolidated, and the tube is collapsed and sealed into a preform. During the collapsing process, red emission can be seen clearly at a certain high temperature. After the preform is collapsed, its core area exhibits a light brown color, with white paper used as a background.

The preform refractive index profile (RIP) is acquired using a PK2600 Preform Analyzer (Photon Kinetics) (see Fig. 5(b)). As seen from Fig. 5(b), there is a dip in the center of the fiber preform, which is due to vaporization of GeO_2 and P_2O_5 [41]. The preform diameter is ~11.85 mm, the core diameter is 0.38 mm, and the NA of the preform is 0.19. The estimated concentrations of each ingredient are $[Er_2O_3] \sim 0.01$, $[Al_2O_3] \sim 0.15$, $[Bi_2O_3] \sim 0.16$, $[P_2O_5] \sim 0.94$, and $[GeO_2] \sim 12.9$ mol%, where the concentration of Bi is higher than that in the BDF discussed previously [42,43]. Fiber drawing is performed with a fiber draw tower manufactured by Controls Interface (Fig. 5(a)). The fiber preform is slowly fed into a furnace. The furnace temperature is set at 1920°C. The fiber diameter can be further adjusted by tuning the ratio of the draw speed and feed speed. The bared fiber is then coated with UV-curable coating made by DSM Desotech B. V. Figure 5(c) shows the cross section of the BEDF [44].

The first developed BEDF shows ultra-broadband luminescence between 1000 and 1570 nm, covering the O-, E-, S-, C-, and L-bands, when pumped by 532, 808, or 980 nm lasers [21,45]. Owing to the existence of multiple active sites, the fluorescence profiles are found highly pump-wavelength-dependent, which is associated with different combinations of excitations in both BACs and Er ions. The luminescence BW can be tuned and designed by selecting pump source(s) and simultaneous pumping. We have experimentally confirmed that the underlying process results in the ultra-broadband luminescence shown in Fig. 6 when using two co-propagating pumps (532 and 808 nm) [21]. It is clear that the luminescence excited with dual-pumping (c) is nearly the same as a linear sum of the individual spectra with single-pump excitation (d). The full width at half maximum (FWHM) of the spectra for dual-pumping is ~ 470 nm, from 1100 to 1570 nm, but the flatness still needs to be improved. Nevertheless, the results clearly demonstrate that BEDFs can be used as ultra-broadband gain media for broadband amplified spontaneous emission (ASE) sources, fiber lasers, or amplifiers in telecommunications and other fields.

2.2.2 BEYDF fabrication by MCVD and the *in situ* doping technique

Following the fabrication procedure of BEDFs and the proposed design shown in Fig. 2 [36], a Bi/Er/Yb co-doped silicate fiber (BEYDF) has also been fabricated by co-doping a BEDF with Yb^{3+} using a similar fabrication technique [22,46]. In comparison to BEDFs, BEYDFs exhibit broadened and, at the same time, enhanced emission, as shown in Fig. 7 [22]. In particular, the overall BW corresponding to a 4 dB drop in intensity is $\Delta\lambda$ = (1000–1590) nm in BEYDFs, while in BEDFs it is only $\Delta\lambda$ = (1250–1590) nm. The overall emission intensity is enhanced by a factor of 2.5 in BEYDFs compared to that in BEDFs. Furthermore, the Er^{3+} gain at 1530 nm is increased, and the BAC-related excited state absorption

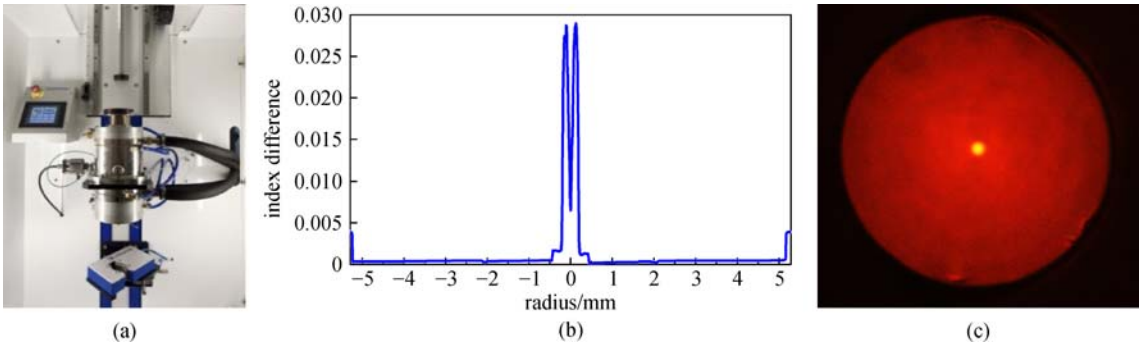

Fig. 5 (a) Customised draw tower, one part of the Joint National Fiber Facility installed at The University of NSW [39]; (b) refractive index of the first BEDF preform fabricated with MCVD and in situ doping technique; (c) cross section of a BEDF

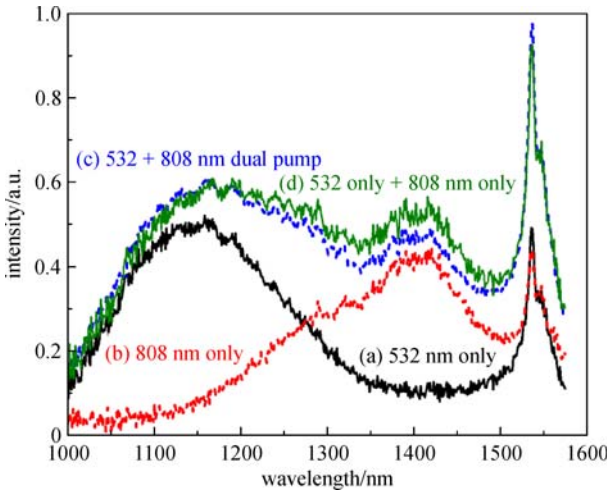

Fig. 6 Emissions of a BEDF pumped by (a) 532 nm only (solid black); (b) 808 nm only (solid red); (c) dual pumping (both 532 and 808 nm (dashed blue). For comparison, the direct addition of the emissions by 532 nm only and by 808 nm only is shown as (d) (solid green) [21]. (Here the BEDF fiber length: 14 cm; 532 nm pump: 92 μW; 808 nm pump: 188 μW)

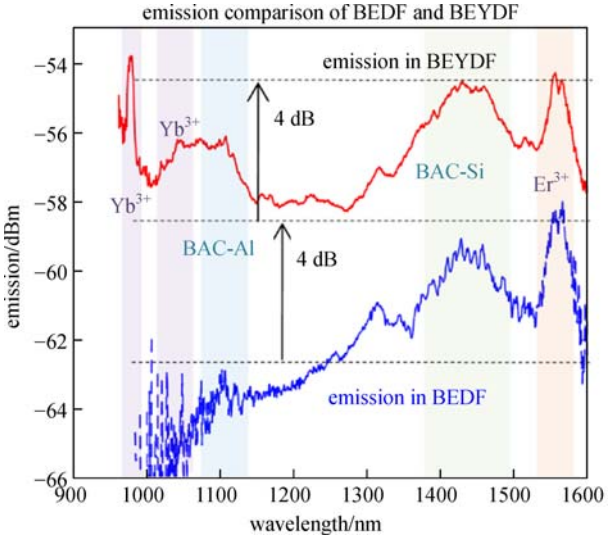

Fig. 7 Emission comparison of BEYDF and BEDF measured under 40 mW 830 nm pumping [22]

(ESA) at 1400 nm is reduced in BEYDFs. The Yb^{3+}-related emission and energy transfer from the excited Yb^{3+} to both the Er^{3+} ions and BACs can explain the improvements in the emission and gain. These results indicate that Yb^{3+} co-doping can be used to expand and enhance the broadband emission and gain of BEYDFs [22].

2.2.3 BDF fabrication by MCVD and the ALD technique

In collaboration with Shanghai University, we also developed a combined technique of MCVD and ALD for BDF fabrication [47]. ALD is a chemical vapor deposition technique based on sequential use of self-terminating gas–solid reactions, which represents a self-limiting surface reaction with advantages including its good uniformity, favorable dispersibility, and high doping concentration as a novelty [47]. The fabrication process can be divided into four steps: firstly, a porous soot layer is deposited on the inner side of the substrate tube using MCVD and then sintered into a semi-clear soot layer; secondly, Bi and Al ions are introduced on the surface of the porous soot layer using the ALD technique (TFS-200, Beneq, Finland), with bis(2,2,6,6-tetramethyl-3,5-heptanedionato) bismuth(III) ($Bi(thd)_3$) and H_2O as Bi and O precursors and with $Al(CH_3)_3$(TMA) as an Al precursor, respectively; thirdly, a germanium optical fiber core layer is doped using MCVD, and a Bi/Al co-doped optical fiber preform with a Ge-doped higher-index core is formed by the MCVD collapsing process; lastly, the preform is drawn into fibers. Under 532 nm pumping, the fabricated BDFs display clear fluorescence bands at 600–850 nm and 900–1650 nm [47]. The maximum fluorescence intensity is located at 1120 nm and attributed to BAC-Al emission, with a FWHM of ~180 nm.

2.3 Optical characterization

For characterization of the active fibers with ultra-broadband spectroscopic properties, in addition to the traditional techniques, we developed several new measurement techniques, including simultaneous measurement of the emission and absorption spectra of the active optical fibers by direct side-pumping [36], tunable laser sources (TLS) based excitation–emission spectroscopy [37,48], and fluorescence lifetime (FLT) measurements using traditional time-domain spectroscopy and modern digital signal processing (DSP) [49,50].

2.3.1 Simultaneous measurements of emission and absorption by side-pumping

Emission and absorption are two key properties of active optical fibers that are important for evaluating and utilizing these fibers and waveguides in various applications, such as fiber amplifiers and lasers. Spectral emission measurements usually employ co- or counter-pumping schemes. The latter is preferred since, in the former, the residual pump power can be significant, resulting in strong background noise. However, ultra-broadband emission measurements in the counter-pumping scheme are also limited by the availability of a broadband WDM coupler. In addition, for an intrinsic emission measurement, a shorter fiber is preferred, since it allows minimizing the influence of the fiber length [36]. For example, traditional absorption measurements based on the cutback method involve fiber cutting, so the accuracy can be easily affected

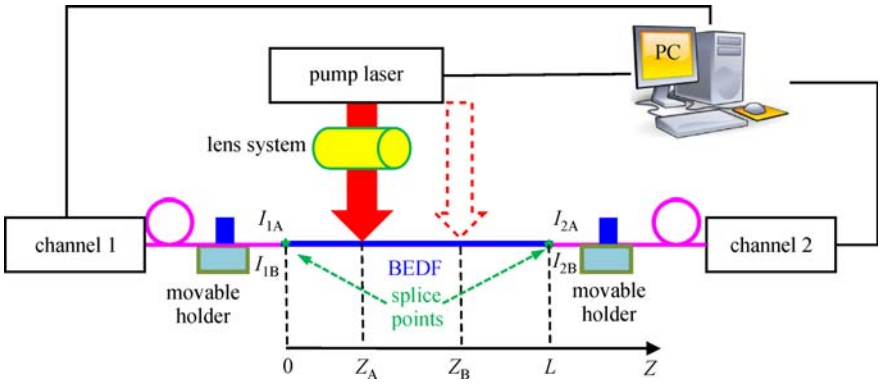

Fig. 8 Configuration of the simultaneous emission and absorption measurement of active optical fiber by side pumping and the related coordinate system

by the uncertainty in cutting, re-splicing, or realigning [36]. In this context, a direct side-pumping scheme (Fig. 8) is proposed for non-destructive evaluation of active optical fibers [36]. This scheme is free from fiber cutting and provides intrinsically low pump background and simultaneous accurate measurement of emission and absorption. The absorption of BEDFs can be extracted from the emission spectra (Channel 1: I_{1A}, I_{1B}, Channel 2: I_{2A}, I_{2B}) obtained in two measurements at two different positions Z_A and Z_B in Fig. 8 and expressed as [36]

$$\alpha(\lambda) = \frac{\ln\left[\frac{I_{1A}(\lambda) \times I_{2B}(\lambda)}{I_{1B}(\lambda) \times I_{2A}(\lambda)}\right]}{2(Z_B - Z_A)}. \quad (1)$$

The feasibility of the proposed method is proved by measuring a commercialized EDF. In particular, the robustness of the method is demonstrated by obtaining matching results on a non-perfect BEDF that has a 5 μm off-axis shift in the fiber core and an emission bandwidth of over 300 nm. We expect this method to become a standard measurement scheme for various types of active optical fibers [36].

2.3.2 Combined excitation–emission spectroscopy based on TLS

It is known that combined excitation–emission spectroscopy allows construction of contour plots of the dependencies on λ_{em} and λ_{ex} and is a powerful tool for identifying BACs in BDFs [51]. The fluorescence profiles of BACs in BEDFs are highly pump-wavelength-dependent suggesting the presence of two or more Bi defect centers [21]. Therefore, it is necessary to obtain more information by simultaneous emission and excitation measurements. Based on two Agilent tunable laser systems (Agilent tunable laser measurement system 8164B/81600B-130: 1260 to 1375 nm, low-SSE and 8164B/81600B-140: 1370 to 1495 nm, low-SSE) and an Agilent optical spectrum analyzer (OSA), simultaneous emission and excitation measurements have been performed, with the excitation–emission spectrogram of a typical BEDF shown in Fig. 9 [37,48]. As seen from Fig. 9, there are two apparent emission bands with their central wavelengths at 1420 and 1530 nm, which are related to BAC-Si and Er^{3+}, respectively.

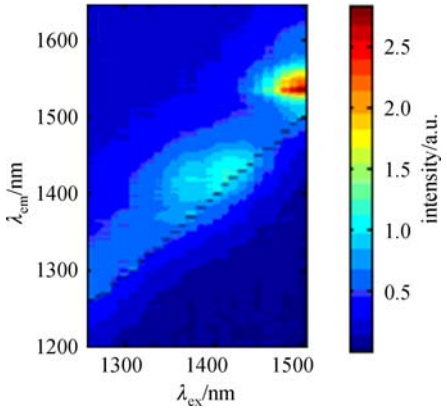

Fig. 9 Excitation-emission spectrogram of a typical BEDF [37]

2.3.3 FLT measurements by traditional time-domain spectroscopy and DSP

FLT is another important performance parameter of doped fibers [52]. The lifetime depends strongly on the presence of dopants such as Er, Bi, Tm, Yb, and Pr ions, host materials such as silica glasses, and fabrication techniques [52,53]. BACs in BEDFs are sensitive to the dopant concentrations and material composition, which results in variations of the emission parameters such as the FLT. An accurate and convenient scheme for the FLT measurements of complex emission processes with either single or multiple FLTs is essential. We developed a new convolution-based scheme for the FLT measurements shown in Fig. 10, which consists of a laser diode (LD), monochromator (MONO), chopper, photo detector, oscilloscope

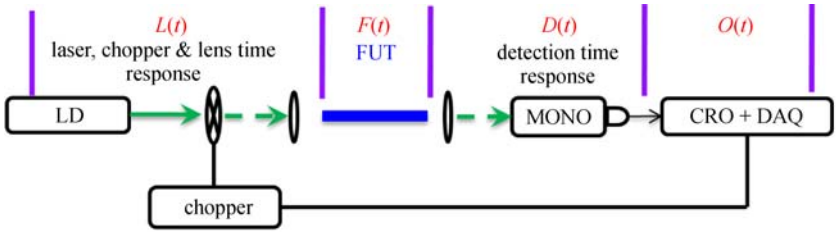

Fig. 10 Schematic of FLT measurement with traditional time-domain spectroscopy and modern DSP

(CRO), and data acquisition module (DAQ) [49,50]. As seen from Fig. 10, the time domain signal ($O(t)$) acquired by the oscilloscope is given by

$$O(t) = L(t) \otimes F(t) \otimes D(t), \tag{2}$$

where $L(t)$ is the combined time response function of the laser, chopper, and lens, $F(t)$ is the time response of the fiber under test (FUT), and $D(t)$ is the detection time response. We then perform the two following tests.

1) The reference test: a passive fiber is used as the FUT, and the reference signal, $O_r(t)$, is given by [49,50]

$$O_r(t) = L(t) \otimes F_r(t) \otimes D(t). \tag{3}$$

For the passive fiber without fluorescence, $F_r(t) = \delta(t)$, so $O_r(t)$ becomes

$$O_r(t) = L(t) \otimes D(t). \tag{4}$$

2) The emission test: an active fiber is used as the FUT, and the emission signal, $O_e(t)$, is given by [49,50]

$$\begin{aligned} O_e(t) &= L(t) \otimes F_e(t) \otimes D(t) \\ &= \Big(L(t) \otimes D(t)\Big) \otimes F_e(t), \end{aligned} \tag{5}$$

where $F_e(t)$ is the impulse response of the active fiber with fluorescence.

After substituting Eq. (4) into Eq. (5), $O_e(t)$ becomes

$$O_e(t) = O_r(t) \otimes F_e(t). \tag{6}$$

After performing the emission and reference tests, $F_e(t)$, which contains the FLT, can be extracted by the DSP algorithm through a convolution method. The FLT results on BEDFs and EDFs are in good agreement with the values reported in other works and prove the capability of the proposed scheme for accurate and repeatable FLT measurements with either single or dual time constants and in a wide range of FLTs. The novelty of the proposed scheme lies in the combination of convolution-based DSP algorithms with a low-cost and simple time-domain spectroscopic setup. The convolution-based scheme is able to achieve accurate microsecond FLT resolution using a spectroscopic setup with only millisecond-scale FLT resolution, for both single and multiple FLTs [49,50].

2.4 Key performance assessment

2.4.1 Role of Bi and Er co-doping in the broadband emission

To investigate the effect of Bi and Er on the emission, short fiber samples with varying Bi and Er concentrations were fabricated (BEDF1, BEDF2, and BEDF3). The samples were pumped by an 830 nm laser diode with a power of 60 mW, and the emission was measured, as shown in Fig. 11 [37]. As seen from Fig. 11, the emission at 1530 nm clearly increases with the increasing concentration of Er ions. The emission around 1200 nm also increases when the Er^{3+} concentration is increased. In particular, it is found that the emission band is the narrowest, and the emission between 1000 and 1300 nm is weaker, whereas there is no clear Er emission at 1530 nm from BEDF3 without Er^{3+}, indicating the dependence of the emission between 1000 and 1300 nm upon the presence of Er ions and possible energy transfer from Er ions to BACs. Thus, Er co-doping improves not only the C-band and L-band but also the O-band emission.

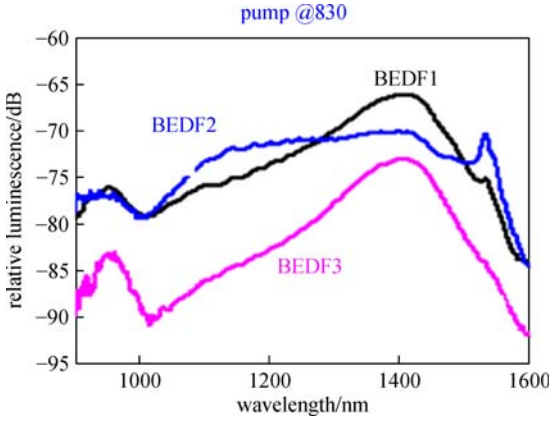

Fig. 11 Luminescence of BEDF with different Bi and Er concentrations. Here luminescence from 1 cm fiber samples is obtained by an 830 nm laser at 60mW. BEDF1: Bi_2O_3~0.05 mol%, $Er_2O_3 < 0.005$ mol%; BEDF2: Bi_2O_3~0.02 mol%, Er_2O_3~0.01 mol%; BEDF3: Bi_2O_3~0.01 mol%, Er_2O_3~0 mol%. The concentrations of other dopants are ~ 0.15 mol% [Al_2O_3], ~0.94 mol% [P_2O_5] and ~12.9 mol% [GeO_2], respectively [37]

The emission BW is not significantly affected by the Bi concentration. However, stronger emission at 1420 nm can be observed for a fiber with higher Bi concentration and, more importantly, stronger emission at 1200 nm can be observed for BEDF2 with higher Er co-doping. The stronger emission at 1200 nm in BEDF2, as compared to the BEDFs with little or no Er co-doping, may be explained by the energy transfer between BACs and Er ions. In addition, the higher Bi concentration leads to higher absorption, including both small-signal absorption and saturation absorption. Especially, the higher saturation absorption for higher Bi concentration under pumping with 830 nm could be linked to ESA and other Bi-related saturation absorption processes [37].

2.4.2 Role of Al co-doping in the broadband emission

It is known that Al is an important co-dopant used to increase the dopant solubility of rare-earth ions and Bi in BDFs, BEDFs, and EDFs [54]. In BDFs, Al is thought to produce NIR emission presumably through the formation of BAC-Al [5,55,56]. Lasing in BDFs with Al co-doping has been reported. However, the optical gain and the lasing efficiency of BDFs co-doped with Al are much lower compared to those of the amplifiers and lasers made from BDFs co-doped with Ge and P [57]. Such differences are mainly ascribed to the different efficiency of different BACs. Similarly to the case of BDFs, these BACs will also have different contributions to the ultra-broadband emission in BEDFs. In particular, the characteristics of BAC-Al have been identified and assessed from the absorption, emission, ESA, and up-conversion measurements in BEDFs [58]. Absorption at ~1050 nm and emission at 1100 nm of BEDFs were identified and ascribed to BAC-Al. In addition, the broad ESA in BEDFs centered at 1030 nm under 830 nm pumping was also attributed to BAC-Al. Specifically, the 1030 nm ESA originated from the energy level of BAC-Al that produces the emission at 1100 nm significantly affects the 1100 nm emission. The 1100 nm emission energy level of BAC-Al was found to be directly associated with significant ESA at 830 nm, resulting in up-conversion at 532 nm. Therefore, Al co-doping should be reduced when BEDFs are fabricated for operating with 830 nm pumping for ultra-broadband applications covering the 1030 nm wavelength [58].

2.4.3 Clear identification of multiple BACs in BEDF

As mentioned above, the ultra-broadband emission of BEDFs is mainly attributed to the co-existence of multiple BACs. Therefore, it will be useful to identify the characteristics of each BAC. First, the emission spectrum was measured and fitted with multiple Gaussian functions as shown in Fig. 12 [59]. Then, FLTs at some typical wavelengths were tested with the method described in Section 2.3.3; the results are shown in Fig. 12 as well. Through a comparison between the FLTs and Gaussian components, four types of BACs were confirmed and identified as BAC-Si, BAC-Al, BAC-P, and BAC-Ge in BEDFs (Fig. 12).

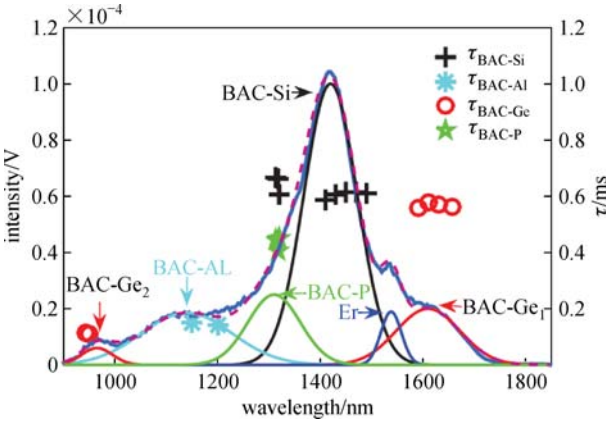

Fig. 12 Emission spectrum of experimental test, Gaussian components, and corresponding FLTs [55]

2.4.4 Efficiency comparison for different pumping

The results in Fig. 4, 6, 7, 9, 11, and 12 clearly demonstrate the existence of multiple active centers in BEDFs, in addition to Er^{3+}. So the fluorescence profiles, as well as efficiency, will be highly pump-wavelength-dependent. The former is discussed in detail in the literature [21,45]. Under 532 or 980 nm pumping, the fluorescence of BEDFs shows two distinct bands at 1130 nm and 1537 nm associated with BAC-Al and Er^{3+}. Under 808 nm pumping, the fluorescence of BEDFs shows two distinct bands at 1400 and 1537 nm associated with BAC-Si and Er^{3+}. Furthermore, the efficiencies under 532, 808 (830), and 980 nm pumping have also been measured using dual-pumping schemes [45,60]. By comparison of the emission integrated from 950 to 1570 nm, it was demonstrated that the emission efficiency of BEDFs under 532 nm (150 μW) pumping is about 1.7 times higher than that under 808 nm (188 μW) pumping [45]. Similarly, the efficiency of the BEDF emission under 830 nm pumping is about 1.8 times higher than that under 980 nm pumping [60]. Therefore, the pumping efficiency for the NIR emission at different pumping wavelengths is in the following order: 532 nm > 808 nm (830 nm) > 980 nm.

2.5 Property modification

Post-treatment of optical fibers and fiber devices by high-temperature annealing, γ-radiation, and laser processing is commonly used to modify the material properties and improve the functionality and stability of the fibers [61–68]. In particular, BACs in bismuth-doped glasses and

fibers have been found to be sensitive to the post-treatment processes such as thermal treatment, γ-radiation, H_2-loading, etc. [15,69–73]. To improve and modify the performance, functionality, and stability, BEDFs have been post-treated by high temperature, γ-radiation, and 830 nm laser radiation.

2.5.1 High-temperature annealing

It is known that the fiber fabrication processes (both the MCVD and fiber drawing processes) are performed under ultra-high temperatures, over 2000°C. Such high-temperature processing results in the formation of bismuth with different valence states and defect sites and therefore different BACs, which affect the NIR emission. Hence, it gives the possibility of controlling BACs through post-treatment under high temperatures and fabricating doped fibers with high fluorescence efficiencies. Based on these considerations, BEDF samples were annealed under different high temperatures, and their emission was measured, with the results shown in Fig. 13 [62]. The results show that the emission of BAC-Si at 1420 nm is significantly decreased for annealing under 100°C–650°C, indicating that BAC-Si-like E' centers may decay at relatively low temperature. Through the comparison of the cross section of the BEDFs without annealing and those annealed at 800°C shown in Fig. 13 [62], the thermal darkening effect is confirmed, which is the main reason for the emission quenching at the annealing temperature of 700°C–800°C. Such thermal darkening effect is believed to be linked to the precipitation of metallic bismuth nanoparticles [73]. These preliminary experimental results further indicate that annealing under temperatures lower than 800°C has negative effect on the BEDF emission, while higher-temperature annealing is proposed to improve the performance of BEDFs.

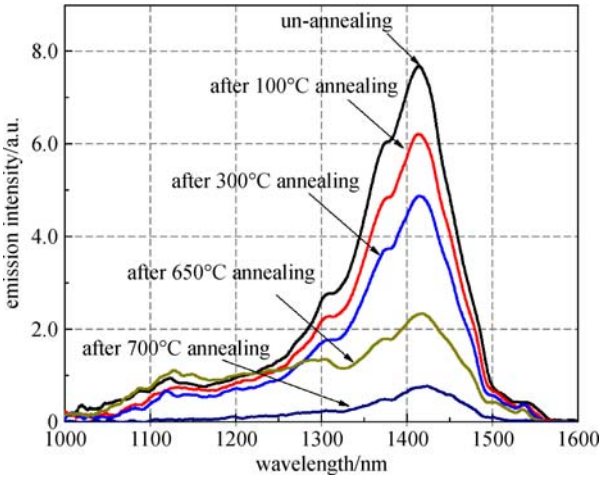

Fig. 13 Progressive emission spectra after annealing processes at different temperature and cross-section of the un-annealed and 800°C annealed (5 h) BEDF (~ 2 cm) [62]

2.5.2 γ-irradiation

Radiation techniques, already established in materials processing, have properties uniquely suited for the creation of new advanced materials. With γ-irradiation from 1.0 to 50 kGy, the absorption at 830 nm is increased significantly, while the absorption at longer wavelengths is reduced, and the corresponding emission is inhibited [59,61,70]. Further investigations on γ-irradiated BEDFs indicate the following [65]:

1) high reliability of BEDFs under low and medium irradiation doses, at quite high dose rates;

2) an increase of the optical transmission over the spectral range of 900–1650 nm under γ-irradiation up to a dose of 15 kGy;

3) an increase of the ratio between the saturable and unsaturable absorption at 830 nm by γ-irradiation, leading to an improved emission efficiency;

4) the existence of some design properties (related to the fiber composition and dosage) that can be exploited to improve the performance and photoluminescence characteristics of Bi doped/co-doped fibers.

In addition, through a comparison of the absorption changes before and after irradiation, it has been demonstrated that γ-radiation could help activate inactive bismuth centers into BAC-Si in both BEDFs and BEYDFs. Evidently, co-doping with Yb considerably enhances the γ-radiation-induced effect [63,74].

Similar phenomena have also been observed in BDFs via ALD [64]. After the irradiation, the intensities of the optical fiber absorption peaks at 458, 510, 700, and 800 nm were clearly increased with the increasing radiation dose (0–3.0 kGy). In addition, a new absorption peak appeared at ~580 nm, which may be associated with Al-OHCs. When fiber samples were excited at 532 nm, the intensity of the NIR emission slightly decreased for the fibers irradiated with 1.0, 2.0, and 3.0 kGy. However, when the fiber samples were excited at 980 nm, the fluorescence intensity increased significantly with the increase of the radiation dose (0–2.0 kGy) and then decreased for the radiation dose from 2.0 to 3.0 kGy. Furthermore, the fluorescence intensity of the 1410 nm band (BAC-Si) increased much more than that of the 1150 nm band (BAC-Al).

2.5.3 Laser radiation

The interaction between light and matter enables materials processing to be performed athermally. Laser material processing has seen tremendous progress and is now at the forefront of industrial and medical applications. The activation and enhancement of emission has already been observed in bismuth-doped glasses and fibers by UV [75,76] or femtosecond laser [71] radiation. In BEDFs, a reversible photo-bleaching effect has been observed as shown in Fig. 14 [68]. Irradiation by 830 nm laser light

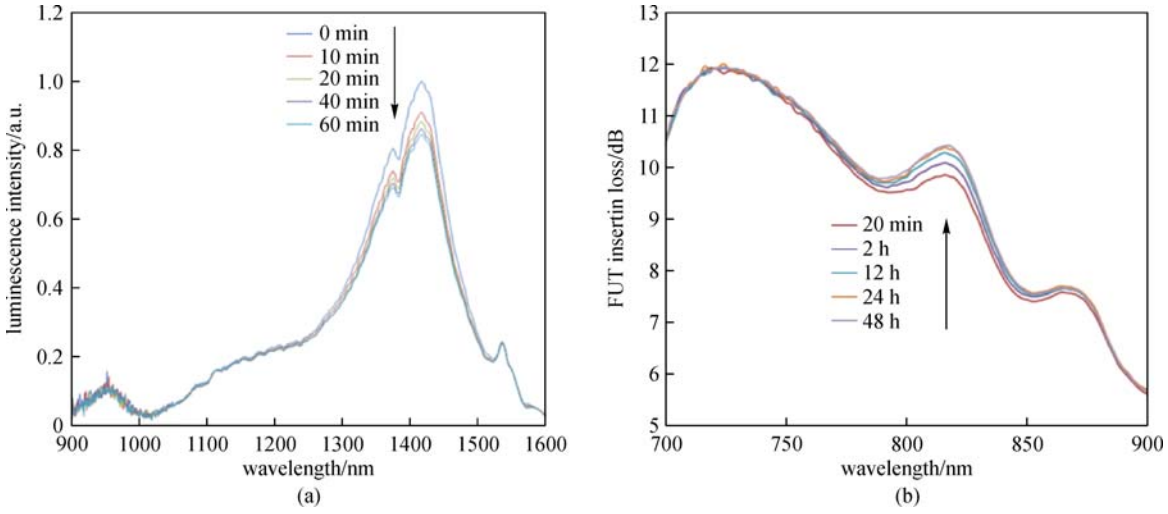

Fig. 14 (a) Luminescence of the FUT under 830 nm pump of 60 mW as a function of time; (b) attenuation of FUT as a function of time after 1 h irradiation of 830 nm pump at 60 mW in the range of 700–900 nm [68]

reduces the emission at ~1420 nm (Fig. 14(a)) and the absorption at ~816 nm (the recovery process in Fig. 14(b)), indicating a photo-bleaching effect of BAC-Si by 830 nm laser radiation [68]. Further results show that the bismuth-related luminescence can be partially bleached by irradiation with 830 nm laser light, and totally recovers to the original level after the irradiation is terminated. A detailed analysis indicates that this reversible bleaching is possibly caused by the electron migration between Bi ions in BAC-Si and the defects or ligands nearby.

2.6 Photonic applications

2.6.1 Ultra-broadband emission source

Broadband light sources have numerous applications in spectral measurements of optical fiber devices and systems. Modern commercial broadband sources, like Xenon lamps and supercontinuum light sources, have various limitations for photonic applications [37]. Therefore, the development of cheap and stable broadband fiber sources is still a hot and urgent topic. The ultra-broadband emission of BEDFs offers a possibility of using them as broadband light sources. The luminescence spectrum emitted from a 3 m BEDF under a pump power of ~ 60 mW and measured by the OSA with a 5 nm BW is shown in Fig. 15 [37,77]. The spectral intensity after compensation of the WDM transmission loss is over −45 dBm from 1100 to 1570 nm and over −50 dBm from 900 to 1100 nm. This intensity is > 10 dB stronger than that of the normal white light source coupled into a single-mode fiber, such as Xenon lamps and some commercialized white light sources with single mode fiber outputs (AQ4305).

A typical application of such broadband light source is for an ultra-large fiber sensing network. Combining the

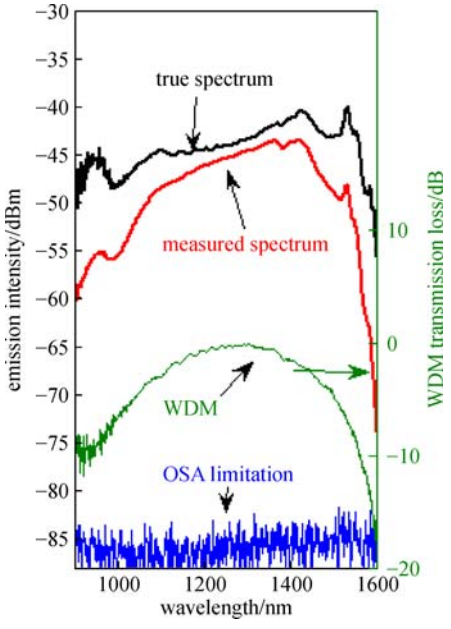

Fig. 15 Broadband emission of 3 m BEDF under 60 mW 830 nm pumping [37]

ultra-broadband emission from BEDFs with general fiber Bragg gratings (FBGs), an ultra-large distributed fiber sensing network can be constructed. Figure 16 shows the transmission spectrum of 4 cascaded FBGs based on BEDFs, where the largest difference of the Bragg wavelength is over 250 nm from 1286 to 1544 nm. If the channel bandwidth of each FBG is assigned as 1 nm, the number of multiplexed fiber gratings is up to 250. If the time-division multiplexing (TDM, ×16) and spatial division multiplexing (SDM, ×8) techniques are further considered, in theory, an ultra-large fiber sensing network

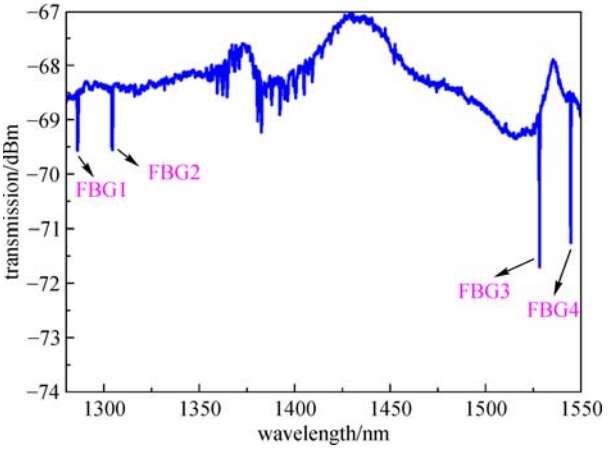

Fig. 16 Ultra broadband transmission spectrum of cascaded 4 fiber Bragg gratings based on BEDF

with up to 32000 sensing units can be constructed. It is far larger than current sensing networks, which is very useful and profitable for various sectors of the economy, society, and military.

2.6.2 Optical amplification

The goal of the BEDF development is to obtain appropriate optical fiber amplifiers to fully utilize the telecommunications transmission window in the range of 1150–1700 nm. In addition to the demonstration of the ultra-broadband emission in the extended bands, significant broadband gain is measured between 1350 and 1470 nm with less than 10 mW of 830 nm pump power, as shown in Fig. 17 [78]. As seen from Fig. 17, with a pump power of 2.58 mW, the peak gain coefficient is > 3 dB/m. It increases to > 4 dB/m for a pump power of 9.41 mW. For higher powers, the broadband gain saturates. The recent work by Firstov et al. has also demonstrated gain bandwidth over 200 nm ranging from 1530 to 1770 nm for 1460 nm laser pumping in BEDFs [79].

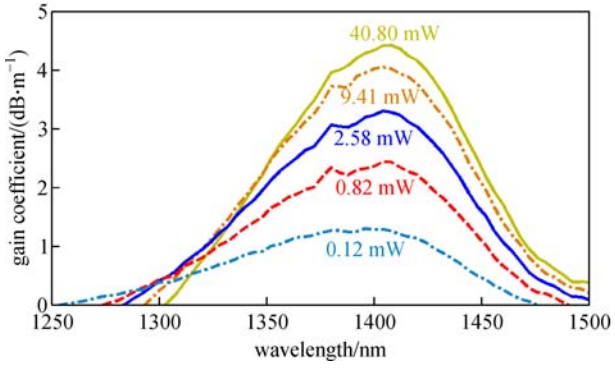

Fig. 17 Gain spectra of the BEDF (52 cm) with different 830 nm pump power [78]

2.6.3 Photosensitivity and gratings

FBGs are important components for fiber sensing and fiber lasers. Efficient inscription of Bragg gratings in BEDFs with and without H_2 loading has been demonstrated with both 193 nm ArF [66] and 244 nm Ar^+ [67] lasers. The photosensitivity of BEDFs has been studied by the Bragg gratings inscription process, and the results show that the photosensitivity of BEDFs at 244 nm is comparable to that of boron-co-doped germanosilicate fibers (GF1) [67]. This is consistent with the fact that they have similar levels of GeO_2, and both are produced by MCVD. In addition, the evolution in the index modulation of BEDFs by 193 nm laser light behaves in a very complex way. Good thermal stability is obtained with H_2 loading [66].

2.6.4 DFB laser

The broadband emission of BEDFs provides the possibility of fabricating fiber lasers across the O-, E-, S-, C-, and L-bands, if a suitable lasing configuration is used. Although fiber lasers operating at O-, E-, and S-bands are more desirable, in a proof-of-principle study, the simplest distributed feedback (DFB) laser at 1.5 μm, which is formed by using π-phase-shifted FBGs written continuously over the length of BEDFs, has been proposed. With the demonstrated photosensitivity of BEDFs at 244 nm, a DFB laser based on phase-shifted gratings without apodization was fabricated, with the DFB fiber laser spectrum (resolution bandwidth = 0.06 nm) peaked at 1538.075 nm with a FWHM of 0.08 nm under 70 mW pumping [67].

3 Summary

Based on several sophisticated fiber fabrication techniques, including combinations of MCVD and in situ solution doping or MCVD and ALD, BDFs, BEDFs, and BEYDFs have been successfully fabricated. Ultra-broadband emission of BEDFs from 1100 to 1550 nm and that of BEYDFs from 1000 to 1590 nm have been demonstrated. According to the analysis of the absorption, emission, on–off gain, ESA, and FLT, four types of BACs (BAC-Si, BAC-Ge, BAC-P, and BAC-Al) have been identified in BEDFs. It has been found that BAC-Al has an adverse effect on the ultra-broadband emission with 830 nm pumping, which suggests that Al co-doping should be reduced. In addition, there is evidence for energy transfer between BACs and Er or Yb active centers. Many fundamental scientific and technological issues and challenges still remain, for example, the unknown origin of BACs and their formation condition and control, evaluation standards for such special active optical fiber, and further improvement of the performance of fiber lasers and amplifiers. Never-

theless, several photonic applications for broadband light sources, amplification, and DFB lasers have already demonstrated the great potential of BEDFs as advanced active laser media for O-, E-, S-, C-, and L-bands.

Acknowledgements Authors are thankful for the support of National Natural Science Foundation of China (Grant Nos. 61520106014, 61405014 and 61377096), Key Laboratory of In-fiber Integrated Optics, Ministry Education of China, State Key Laboratory of Information Photonics and Optical Communications (Beijing University of Posts and Telecommunications) (No. IPOC2016ZT07), Key Laboratory of Optical Fiber Sensing & Communications (Education Ministry of China), Key Laboratory of Optoelectronic Devices and Systems of Ministry of Education and Guangdong Province (No. GD201702) and Science and Technology Commission of Shanghai Municipality, China (Nos. SKLSFO2015-01 and 15220721500). We also wishes to express our thanks to all members of Photonics & Optical Communications at UNSW, Prof. John Canning and Dr. Kevin Cook at University of Sydney, Prof. Graham Town at Macquarie University, and Prof. Tingyun Wang at Shanghai University for their assistance and contributions.

References

1. Richardson D J, Fini J M, Nelson L E. Space-division multiplexing in optical fibres. Nature Photonics, 2013, 7(5): 354–362
2. Dianov E M. Amplification in extended transmission bands using bismuth-doped optical fibers. Journal of Lightwave Technology, 2013, 31(4): 681–688
3. Won R. View from... communication networks beyond the capacity crunch: is it crunch time? Nature Photonics, 2015, 9(7): 424–426
4. https://en.wikipedia.org/wiki/Optical_amplifier
5. Fujimoto Y, Nakatsuka M. Infrared luminescence from bismuth-doped silica glass. Japanese Journal of Applied Physics, 2001, 40 (Part 2, No. 3B): L279–L281
6. Ohkura T, Fujimoto Y, Nakatsuka M, Young-Seok S. Local structures of bismuth ion in bismuth-doped silica glasses analyzed using Bi LIII X-ray absorption fine structure. Journal of the American Ceramic Society, 2007, 90(11): 3596–3600
7. Fujimoto Y. Local structure of the infrared bismuth luminescent center in bismuth-doped silica glass. Journal of the American Ceramic Society, 2010, 93(2): 581–589
8. Sokolov V O, Plotnichenko V G, Koltashev V V, Dianov E M. Centres of broadband near-IR luminescence in bismuth-doped glasses. Journal of Physics D, Applied Physics, 2009, 42(9): 095410
9. Meng X G, Qiu J R, Peng M Y, Chen D P, Zhao Q Z, Jiang X W, Zhu C S. Near infrared broadband emission of bismuth-doped aluminophosphate glass. Optics Express, 2005, 13(5): 1628–1634
10. Sun H T, Zhou J, Qiu J. Recent advances in bismuth activated photonic materials. Progress in Materials Science, 2014, 64: 1–72
11. Murata K, Fujimoto Y, Kanabe T, Fujita H, Nakatsuka M. Bi-doped SiO_2 as a new laser material for an intense laser. Fusion Engineering and Design, 1999, 44(1–4): 437–439
12. Dianov E M. Bismuth-doped optical fibres: a new breakthrough in near-IR lasing media. Quantum Electronics, 2012, 42(9): 754–761
13. Riumkin K E, Melkumov M A, Bufetov I A, Shubin A V, Firstov S V, Khopin V F, Guryanov A N, Dianov E M. Superfluorescent 1.44 μm bismuth-doped fiber source. Optics Letters, 2012, 37(23): 4817–4819
14. Dvoyrin V V, Mashinsky V M, Dianov E M, Umnikov A A, Yashkov M V, Guranov A N. Absorption, fluorescence and optical amplification in MCVD bismuth-doped silica glass optical fibres. In: Proceedings of ECOC, 2005, 4: 949–950
15. Dianov E M. Nature of Bi-related near IR active centers in glasses: state of the art and first reliable results. Laser Physics Letters, 2015, 12(9): 095106
16. Dianov E M. Fiber for fiber lasers: bismuth-doped optical fibers: advances in an active laser media. Laser Focus World, 2015, 51(9): 16
17. Kuwada Y, Fujimoto Y, Nakatsuka M. Ultrawideband light emission from bismuth and erbium doped silica. Japanese Journal of Applied Physics, 2007, 46(4A): 1531–1532
18. Peng M, Zhang N, Wondraczek L, Qiu J, Yang Z, Zhang Q. Ultrabroad NIR luminescence and energy transfer in Bi and Er/Bi co-doped germanate glasses. Optics Express, 2011, 19(21): 20799–20807
19. Minh Hau T, Yu X, Zhou D, Song Z, Yang Z, Wang R, Qiu J. Super broadband near-infrared emission and energy transfer in Bi–Er co-doped lanthanum aluminosilicate glasses. Optical Materials, 2013, 35(3): 487–490
20. Minh Hau T, Wang R, Yu X, Zhou D, Song Z, Yang Z, He X, Qiu J. Near-infrared broadband luminescence and energy transfer in Bi–Tm–Er co-doped lanthanum aluminosilicate glasses. Journal of Physics and Chemistry of Solids, 2012, 73(9): 1182–1186
21. Luo Y, Wen J, Zhang J, Canning J, Peng G D. Bismuth and erbium codoped optical fiber with ultrabroadband luminescence across O-, E-, S-, C-, and L-bands. Optics Letters, 2012, 37(16): 3447–3449
22. Sathi Z M, Zhang J, Luo Y, Canning J, Peng G D. Improving broadband emission within Bi/Er doped silicate fibres with Yb co-doping. Optical Materials Express, 2015, 5(10): 2096–2105
23. Wen J, Wang T, Pang F, Zeng X, Chen Z, Peng G D. Photoluminescence characteristics of $Bi^{(m+)}$-doped silica optical fiber: structural model and theoretical analysis. Japanese Journal of Applied Physics, 2013, 52(12R): 122501
24. Corbett J D. Homopolyatomic ions of the post-transition elements—synthesis, structure and bonding. In: Lippard S J, ed. Progress in Inorganic Chemistry. Hoboken, NJ: John Wiley & Sons, Inc., 1976, vol 21
25. Khonthon S, Morimoto S, Arai Y, Ohishi Y. Redox equilibrium and NIR luminescence of Bi_2O_3-containing glasses. Optical Materials, 2009, 31(8): 1262–1268
26. Sun H T, Sakka Y, Gao H, Miwa Y, Fujii M, Shirahata N, Bai Z, Li J G. Ultrabroad near-infrared photoluminescence from $Bi_5(AlCl_4)_3$ crystal. Journal of Materials Chemistry, 2011, 21(12): 4060–4063
27. Sun H T, Sakka Y, Shirahata N, Gao H, Yonezawa T. Experimental and theoretical studies of photoluminescence from Bi_8^{2+} and Bi_5^{3+} stabilized by $[AlCl_4]-$ in molecular crystals. Journal of Materials Chemistry, 2012, 22(25): 12837–12841
28. Sun H T, Yonezawa T, Gillett-Kunnath M M, Sakka Y, Shirahata N, Rong Gui S C, Fujii M, Sevov S C. Ultra-broad near-infrared photoluminescence from crystalline $(K\text{-crypt})_2Bi_2$ containing $[Bi_2]^{2-}$ dimers. Journal of Materials Chemistry, 2012, 22(38): 20175–20178
29. Sun H T, Matsushita Y, Sakka Y, Shirahata N, Tanaka M, Katsuya Y, Gao H, Kobayashi K. Synchrotron X-ray, photoluminescence,

and quantum chemistry studies of bismuth-embedded dehydrated zeolite Y. Journal of the American Chemical Society, 2012, 134(6): 2918–2921

30. Peng M, Dong G, Wondraczek L, Zhang L, Zhang N, Qiu J. Discussion on the origin of NIR emission from Bi-doped materials. Journal of Non-Crystalline Solids, 2011, 357(11-13): 2241–2245
31. Dianov E M, Firstov S V, Melkumov M. Bismuth-doped fiber lasers covering the spectral region 1150–1775 nm. In: Proceedings of Frontiers in Optics 2015, Optical Society of America, San Jose, California, 2015, LTu2H.1
32. Dianov E M, Firstov S V, Melkumov M A. Bismuth-doped optical fibers: advances and new developments. In: Proceedings of Workshop on Specialty Optical Fibers and Their Applications, Optical Society of America, Hong Kong, 2015, WT1A.4
33. https://www.thorlabs.de/newgrouppage9.cfm?objectgroup_id = 1504
34. https://www.thorlabs.de/newgrouppage9.cfm?objectgroup_id = 336
35. Bufetov I A, Melkumov M A, Firstov S V, Riumkin K E, Shubin A V, Khopin V F, Guryanov A N, Dianov E M. Bi-doped optical fibers and fiber lasers. IEEE Journal of Selected Topics in Quantum Electronics, 2014, 20(5): 0903815
36. Zhang J, Luo Y, Sathi Z M, Azadpeyma N, Peng G D. Test of spectral emission and absorption characteristics of active optical fibers by direct side pumping. Optics Express, 2012, 20(18): 20623–20628
37. Zhang J, Sathi Z M, Luo Y, Canning J, Peng G D. Toward an ultra-broadband emission source based on the bismuth and erbium co-doped optical fiber and a single 830 nm laser diode pump. Optics Express, 2013, 21(6): 7786–7792
38. Fukuchi Y, Maeda J. Characteristics of rational harmonic modelocked shortcavity fiber ring laser using a bismuthoxide-based erbiumdoped fiber and a bismuthoxidebased highly nonlinear fiber. Optics Express, 2011, 19(23): 22502–22509
39. http://www2.eet.unsw.edu.au/photonics/NFF.html
40. Webb A S, Boyland A J, Standish R J, Yoo S, Sahu J K, Payne D N. MCVD *in-situ* solution doping process for the fabrication of complex design large core rare-earth doped fibers. Journal of Non-Crystalline Solids, 2010, 356(18-19): 848–851
41. Nagel S R, Macchesney J B, Walker K L. An overview of the modified chemical vapor deposition (MCVD) process and performance. IEEE Journal of Quantum Electronics, 1982, 18(4): 459–476
42. Dianov E M. Amplification in extended transmission bands. In: Proceedings of OFC 2012 OSA, Los Angeles, USA, 2012
43. Razdobreev I, Bigot L. On the multiplicity of bismuth active centres in germano-aluminosilicate preform. Optical Materials, 2011, 33(6): 973–977
44. Peng G D, Luo Y, Zhang J, Wen J, Yan B, Canning J. Recent development of new active optical fibres for broadband photonic applications. In: Proceedings of 4th International Conference on Photonics, IEEE, 2013, 5–9
45. Luo Y, Zhang J, Zareanborji A, Wen J, Canning J, Peng G D. Developing Bi/Er/Al codoped optical fibre with high Bi concentration for ultrabroadband emission. In: Proceedings of 37th Australian Conference on Optical Fibre Technology, Engineering Australian, Sydney, 2012, 117
46. Sathi Z, Yang H, Luo Y, Zhang J, Peng G D. Ytterbium related effects in bismuth/erbium/ytterbium co-doped germanosilicate fibres. In: Proceedings of OptoElectronics and Communications Conference and Australian Conference on Optical Fibre Technology (OECC/ACOFT 2014), IEEE, Melbourne, Australia, 2014, WEPS2–65
47. Wen J, Wang J, Dong Y, Chen N, Luo Y, Peng G D, Pang F, Chen Z, Wang T. Photoluminescence properties of Bi/Al-codoped silica optical fiberbased on atomic layer deposition method. Applied Surface Science, 2015, 349: 287–291
48. Ni J, Peng G D, Wang C, Luo Y, Xiao G, Wei S, Liu H, Liu T. Study on pump optimizing for Bi/Er co-doped optical fiber. Measurement, 2016, 79: 160–163
49. Zareanborji A, Yang H Y, Sathi Z, Luo Y H, Town G, Peng G D. Time-resolved fluorescence measurement based on spectroscopy and DSP techniques for Bi/Er codoped fibre characterization. In: Proceedings of OptoElectronics and Communications Conference and Australian Conference on Optical Fibre Technology (OECC/ACOFT 2014), IEEE, Melbourne, Australia, 2014, TU6C–5
50. Zareanborji A, Yang H Y, Town G, Luo Y H, Peng G D. Simple and accurate fluorescence lifetime measurement scheme using traditional time-domain spectroscopy and modern digital signal processing. Journal of Lightwave Technology, 2016, 34(21): 5033–5043
51. Firstov S V, Khopin V F, Bufetov I A, Firstova E G, Guryanov A N, Dianov E M. Combined excitation-emission spectroscopy of bismuth active centers in optical fibers. Optics Express, 2011, 19 (20): 19551–19561
52. Nykolak G, Becker P C, Shmulovich J, Wong Y H, DiGiovanni D J, Bruce A J. Concentration-dependent $^4I_{13/2}$ lifetimes in Er^{3+}-doped fibers and Er^{3+}-doped planar waveguides. IEEE Photonics Technology Letters, 1993, 5(9): 1014–1016
53. Zhou Y, Gai N, Wang J, Chen F, Yang G. Effect of Ce^{3+}(Eu^{3+}) codoping on the spectroscopic properties of Er^{3+} in bismuth-germanate glass. Optical Materials, 2009, 31(11): 1595–1599
54. Digonnet M J F. Rare-earth-doped fiber lasers and amplifiers. 2nd, devised and expanded. New York: CRC Press, 2002, Chap. 2
55. Bufetov I A, Dianov E M. Bi-doped fiber lasers. Laser Physics Letters, 2009, 6(7): 487–504
56. Fujimoto Y, Nakatsuka M. ^{27}Al NMR structural study on aluminum coordination state in bismuth doped silica glass. Journal of Non-Crystalline Solids, 2006, 352(21–22): 2254–2258
57. Riumkin K E, Melkumov M A, Varfolomeev I A, Shubin A V, Bufetov I A, Firstov S V, Khopin V F, Umnikov A A, Guryanov A N, Dianov E M. Excited-state absorption in various bismuth-doped fibers. Optics Letters, 2014, 39(8): 2503–2506
58. Sathi Z M, Zhang J, Luo Y, Canning J, Peng G D. Spectral properties and role of aluminiumrelated bismuth active centre (BAC-Al) in bismuth and erbium co-doped fibres. Optical Materials Express, 2015, 5(5): 1195–1209
59. Zareanborji A, Luo Y, Peng G D. Characterization and assessment of multiple bismuth active centres in Bi/Er doped fiber. In: Proceedings of 2nd International Conference on Opto-Electronics and Applied Optics (IEM OPTRONIX), 2015, 1–5
60. Yan B, Luo Y, Zareanborji A, Xiao G, Peng G D, Wen J. Performance comparison of bismuth/erbium co-doped optical fibre (BEDF) by 830 nm and 980 nm pumping. Journal of Optics, 2016, 18(10): 105705

61. Canning J, Liu W, Cook K. Annealing and regeneration in optical fibres. In: Proceedings of Asia Communications and Photonics Conference 2015, Optical Society of America, Hong Kong, 2015, AM3C.2
62. Wei S, Luo Y, Ding M, Cai F, Zhao Q, Peng G D. Annealing effects on bismuth active centers in Bi/Er co-doped fiber. In: Proceedings of Conference on Lasers and Electro-Optics, Optical Society of America, San Jose, California, 2016, JTh2A.75
63. Yan B, Luo Y, Sporea D, Mihai L, Negut D, Sang X, Wen J, Xiao G, Peng G. Gamma radiation-induced formation of bismuth related active centre in Bi/Er/Yb co-doped fibre. In: Proceedings of Asia Communications and Photonics Conference 2015, Optical Society of America, Hong Kong, 2015, ASu2A.56
64. Wen J, Liu W, Dong Y, Luo Y, Peng G D, Chen N, Pang F, Chen Z, Wang T. Radiation-induced photoluminescence enhancement of Bi/Al-codoped silica optical fibers via atomic layer deposition. Optics Express, 2015, 23(22): 29004–29013
65. Sporea D, Mihai L, Neguț D, Luo Y, Yan B, Ding M, Wei S, Peng G D. r irradiation induced effects on bismuth active centres and related photoluminescence properties of Bi/Er co-doped optical fibres. Scientific Reports, 2016, 6(1): 29827
66. Cook K, Shao L Y, Canning J, Wang T, Luo Y, Peng G D. Bragg gratings in few-mode Er/Al//Bi/P co-doped germanosilicate ring-core fibre. In: Proceedings of 22nd International Conference on Optical Fiber Sensors, SPIE, Beijing, China, 2012
67. Qi H, Luo Y, Yang H, Zhang J, Canning J, Peng G D. Photosensitivity, phase shifted grating and DFB fibre laser in bismuth/erbium co-doped germanosilicate optical fibre. In: Proceedings of 19th OptoElectronics and Communications Conference, OECC 2014 and the 39th Australian Conference on Optical Fibre Technology, ACOFT 2014, IEEE Computer Society, Melbourne, VIC, Australia, 2014, 495–497
68. Ding M, Wei S, Luo Y, Peng G D. Reversible photo-bleaching effect in Bi/Er co-doped optical fiber. In: Proceedings of Photonics and Fiber Technology 2016 (ACOFT, BGPP, NP), Optical Society of America, Sydney, 2016, ATh2C.3
69. Xu B, Zhou S, Guan M, Tan D, Teng Y, Zhou J, Ma Z, Hong Z, Qiu J. Unusual luminescence quenching and reviving behavior of Bi-doped germanate glasses. Optics Express, 2011, 19(23): 23436–23443
70. Denker B I, Galagan B I, Musalitin A M, Shulman I L, Sverchkov S E, Dianov E M. Alternative ways to form IR luminescence centers in Bi-doped glass. Laser Physics, 2011, 21(4): 746–749
71. Kononenko V, Pashinin V, Galagan B, Sverchkov S, Denker B, Konov V, Dianov E M. Activation of color centers in bismuth glass by femtosecond laser radiation. Laser Physics, 2011, 21(9): 1585–1592
72. Xu J, Zhao H, Su L, Yu J, Zhou P, Tang H, Zheng L, Li H. Study on the effect of heat-annealing and irradiation on spectroscopic properties of Bi:α-BaB_2O_4 single crystal. Optics Express, 2010, 18(4): 3385–3391
73. Wei S, Luo Y, Ding M, Cai F, Xiao G, Fan D, Zhao Q, Peng G D. Thermal effect on attenuation and luminescence of Bi/Er co-doped fiber. IEEE Photonics Technology Letters, 2017, 29(1): 43–46
74. Yan B, Luo Y, Sporea D, Mihai L, Neguț D, Ding M, Wang C, Wen J, Sang X, Peng G D. Enhancing gamma radiation effect in Bi/Er doped optical fibre by co-doping Yb. In: Proceedings of Asia Communications and Photonics Conference 2016, Optical Society of America, Wuhan, China, 2016
75. Ban C, Limberger H G, Bulatov I L, Dvoyrin V V, Mashinsky V M, Dianov E M. Infrared luminescence enhacement by UV-irradiation of H2-loaded Bi-Al-doped fiber. In: Proceedings of ECOC, 2009
76. Violakis G, Limberger H G, Mashinsky V M, Dianov E M. Dose dependence of luminescence increase in H2-loaded Bi-Al co-doped optical fibers by cw 244-nm and pulsed 193-nm laser irradiation. In: Proceedings of OFC, Optical Society of America, 2013
77. Song D, Zhang J, Fang S, Sun W, Sathi Z M, Luo Y, Peng G D. Bismuth and erbium co-doped optical fiber for a white light fiber source. Optics and Photonics Journal, 2013, 3(02): 175–178
78. Yan B, Luo Y, Zareanborji A, Zhang J, Canning J, Peng G D. 1350-1470 nm optical amplification with bismuth/erbium co-doped fibre. In: Proceedings of Australia and New Zealand Conference on Optics and Photonics (ANZCOP) Conference 2013, Engineering Australia, Perth, Australia, 2013
79. Firstov S V, Khopin V F, Riumkin K E, Alyshev S V, Melkumov M A, Guryanov A N, Dianov E M. Bi/Er co-doped fibers as an active medium for optical amplifiers for the C-, L- and U- telecommunication bands. In: Proceedings of ECOC, 2016,1–3

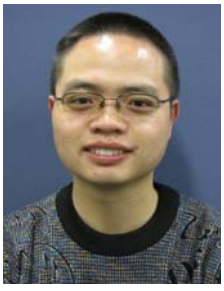

Dr. **Yanhua Luo** received his B.E. and Ph. D. degrees from University of Science and Technology of China (UTSC) in 2004 and 2009, respectively. During his Ph.D. study, he had spent one and a half years in School of Electrical Engineering & Telecommunications at University of New South Wales (UNSW) as a practicum student. His research interest is functional photonics materials, fibers and devices, including rare earth based photonic materials, photo-responsive photonic materials, POF and silica fiber-design, fabrication & applications, etc. He has made many contributions to photonics materials and devices. So far he has held 2 China patents and co-authored 88 refereed journal papers, 70 conference papers and 3 book chapters on these subjects. Dr. Luo started working as a postdoctoral researcher in USTC in 2009 and then in UNSW in 2010. Currently, he works as a lab manager of Photonic & Optical Communications Laboratory at University of New South Wales assisting Prof. Gang-Ding Peng to maintain the National Joint Fibre Facility at UNSW and develop the next generation functional specialty optical fibers and their devices.

Email: yanhua.luo1@unsw.edu.au

A/Prof. **Binbin Yan** received her bachelor's degree in electronic science and technology and her Ph.D. degree in electromagnetic field and microwave technology from Beijing University of Posts and Telecommunications (BUPT), Beijing, China, in 2003 and 2010, respectively. During her Ph.D. study, she had spent two years in School of Electrical Engineering & Telecommunications at University of New South Wales (UNSW) as a practicum

student. In 2010, she joined the institute of Information Photonics and Optical Communications at BUPT as lecturer. From 2016, she is working as an associate professor in the field of new type photonic devices and optical information processing, including fiber amplifier and laser, fiber Bragg grating, optical fiber sensors, photonic crystal fibers, 3D displays, and so on.

Email: yanbinbin@bupt.edu.cn

Prof. **Jianzhong Zhang** received his bachelor's degree of condensed-state physics from the Lanzhou University in 2000 and obtained his master's and doctor's degrees in optical engineering from the Harbin Engineering University in 2004 and 2007, respectively. He then joined the School of Physics at Harbin Engineering University as an A/professor at the end of 2007. He became a full professor of Harbin Engineering University in 2011. During 2006, he visited University of New South Wales (UNSW) as a visiting fellow supervised by Prof. Gang-Ding Peng. His research interests are in optical fiber laser, optical fiber sensors and wave characteristics in periodical structure. He has published more than 60 articles in international journals and conferences. He is currently the PI for six research projects including two funded by the National Natural Science Foundation of China which is ongoing in his parent University.

Email: zhangjianzhong@hrbeu.edu.cn

A/Prof. **Jianxiang Wen** received his M.S. degree in chemical and material engineering from Jiangnan University, Jiangsu, China, in 2006, and received his Ph.D. degree in communication and information systems from Shanghai University, Shanghai, China, and the University of New South Wales, Sydney, Australia, in 2011. From 2001 to 2007, he was an R&D Engineer in Jiangsu Fasten Photonics Company. Now he is an associate Professor, and working at Key Laboratory of Specialty Fiber Optics and Optical Access Networks, Shanghai University. His research interests include design and fabrication in the specialty fiber fields such as spun optical fibers, polarization-maintaining optical fibers, doping fibers (Bi, Pb, Yb, Er, Ce elements), specialty optical fibers with radiation-hardness, and so on, be proficient in MCVD and ALD techniques for the fibers fabrication. His awards include Jiangsu Province Science and Technology Progress Award (Second Prize) in 2008, National Public Postgraduate Award China in 2009.

Email: wenjx@shu.edu.cn

Dr. **Jun He** received his bachelor's degree in electronic science and technology from Wuhan University, Wuhan, China, in 2006 and his Ph.D. degree in electrical engineering from the Institute of Semiconductors, Chinese Academy of Sciences (CAS), Beijing, China, in 2011. From 2011 to 2013, he was with Huawei Technologies Co. Ltd., Shenzhen, China, as a Research Engineer and worked on performance monitoring techniques for agile optical networks. Since 2013, he has been with Shenzhen University, Shenzhen, China, first as a Postdoctoral Research Fellow and then as an Assistant Professor. From 2015 to 2016, he was with the University of New South Wales (UNSW), Sydney, Australia, as a Visiting Fellow. Since 2017, he has been in Shenzhen University, Shenzhen, China, as an Assistant Professor. His current research interests focus on optical fiber sensors, fiber Bragg gratings (FBGs), and fiber lasers. He has authored or coauthored 4 patent applications and more than 50 journal and conference papers. Dr. He is a member of the Optical Society of America.

Email: hejun07@szu.edu.cn

Prof. **Gang-Ding Peng** received his B.Sc. degree in physics from Fudan University, Shanghai, China, in 1982, and M.Sc. degree in applied physics and Ph.D. degree in electronic engineering from Shanghai Jiao Tong University, Shanghai, China, in 1984 and 1987, respectively. From 1987 through 1988, he was a lecturer of the Jiao Tong University. He was a postdoctoral research fellow in the Optical Sciences Centre of the Australian National University, Canberra, from 1988 – 1991. He has been working with UNSW since 1991, was a Queen Elizabeth II Fellow from 1992 – 1996 and is currently a Professor in the same university. He is a fellow and life member of both OSA and SPIE. His research interests include specialty silica and polymer optical fibers, optical fiber and waveguide devices, optical fiber sensors and nonlinear optics. So far, he has published more than 200 refereed journal papers and more than 200 conference papers, and co-authored more than 10 book chapters on these subjects.

Email: g.peng@unsw.edu.au